Nuclear Anomalous Dispersion in Fe^{57} by the Method of Total Reflection

S. BERNSTEIN AND E. C. CAMPBELL
Oak Ridge National Laboratory, Oak Ridge, Tennessee
(Received 19 July 1963)

The recoil-free coherent resonant scattering of the 14.4-keV Fe^{57} gamma rays has been investigated by employing the techniques of the Mössbauer effect together with those of total reflection. Of particular interest are the observed large interference effects attributed to the coherent superposition of the several resonant nuclear contributions and the nonresonant electronic contribution to the scattering amplitude in the forward direction. Gamma rays from a 300-mCi Co^{57} source, diffused into the thin edge of a stainless steel plate, were reflected at small glancing angle θ by an optically flat Fe^{57} mirror through a narrow slit into a NaI scintillation detector. The resonant frequency spectrum of the Fe^{57} nuclei in the mirror was scanned by varying the source velocity v. Values of the absolute reflectivity $R(\theta,v)$ were obtained by comparison of the direct and reflected measured intensities. In an auxiliary experiment $R(v)$ was measured with an external magnetic field applied to the mirror. The results of these measurements were compared with computer-programmed calculations based on the classical optical theory of total reflection. Appropriately averaged quantum-mechanical expressions were introduced for the coherent resonant nuclear scattering amplitude in the forward direction. Separate computations were made for each polarization state of the incident radiation; these were averaged to give $R(\theta,v)$ appropriate for an unpolarized source and a polarization-insensitive detector. Suitable integrations were performed to take into account the frequency spread and angular width of the incident radiation. For $\theta=4$ mrad, $R(v)$, computed with the six resonances of normal ferromagnetic Fe^{57}, agreed in shape and magnitude with the observed reflectivity, when the resonance width was assumed to be four times the natural width. For $\theta=2$ mrad, where the gamma-ray penetration depth is small, anomalies in the magnetic and chemical environment of the Fe^{57} nuclei near the mirror surface required the introduction of additional resonances for FeO and for nonmagnetic Fe.

INTRODUCTION

THE discovery of recoil-free resonant nuclear absorption of gamma rays by Mössbauer,[1] and much of the early work following, involved transmission experiments. The technique of the Mössbauer effect also makes possible the study of resonance scattering of gamma rays from nuclei as a function of frequency, and of the coherent effects of electron and nuclear scattering. Recoil-free resonance scattering of gamma rays by nuclei was first reported by Picou, Barloutaud, and Tzara.[2] Interference effects between the electron scattering and the resonant nuclear scattering were first reported by Black and Moon,[3] who used a multiple-line Fe^{57} source and a polycrystalline normal iron foil scatterer to observe changes in intensity in the direction of one of the Debye-Scherrer rings as a function of the frequency of the gamma rays. During the period of the work of Black and Moon we were studying coherent scattering by observing the total reflection of a single-line Fe^{57} source from a highly enriched Fe^{57} mirror. A brief description of our preliminary work on total reflection has been reported.[4] Further observations of Bragg scattering were reported by Black, Evans, and O'Connor.[5]

This paper is a summary of our work on total reflection. Our primary interest here is the gamma-ray optics involving both atomic electrons and nuclei in a region of nuclear anomalous dispersion. The main optical features of interest are the interference between the contributions to the nuclear-scattering amplitude from the transitions between the several nuclear Zeeman levels, and the interference between the nuclear- and electron-scattering amplitudes. The nuclear-scattering amplitude varies widely with frequency in the region of nuclear resonance scattering; the electron-scattering amplitude is independent of frequency in this narrow region of energy, since it is unlikely that the incident photon energy is close to an x-ray absorption limit of the scatterer. The resultant of the coherent superposition of the resonant nuclear contributions and the nonresonant electronic contribution to the scattering amplitude depends upon the frequency in the resonance region. Evidence for the interference between these contributions is given by the dependence of the mirror reflectivity R upon frequency ν of the incident gamma rays, and upon the glancing angle θ. We describe below our measurements of $R(\nu,\theta)$ and compare these measurements with the values computed from theory.

THEORETICAL CONSIDERATIONS

The reflectivity of the mirror R is given from classical physical optics, by the expression[6]

$$R(z)=\left|\frac{1-(1-z)^{1/2}}{1+(1-z)^{1/2}}\right|^2 \qquad (1)$$

[1] R. L. Mössbauer, Z. Physik **151**, 124 (1958).
[2] R. Barloutaud, J. L. Picou, C. Tzara, Compt. Rend. **250**, 2705 (1960).
[3] P. J. Black and P. B. Moon, Nature **188**, 481 (1960).
[4] S. Bernstein and E. C. Campbell, in *Proceedings of the Second International Conference on the Mössbauer Effect, Saclay, France, 1961* (John Wiley & Sons, Inc., New York, 1961), p. 250.
[5] P. J. Black, D. E. Evans, and D. A. O'Connor, in *Proceedings of the Second Conference on* the *Mössbauer Effect, Saclay, France, 1961* (John Wiley & Sons, Inc., New York, 1961), p. 233.
[6] A. H. Compton and S. K. Allison, *X-Rays in Theory and Experiments* (D. Van Nostrand Company, Inc., New York, 1935), 2nd ed., p. 308.

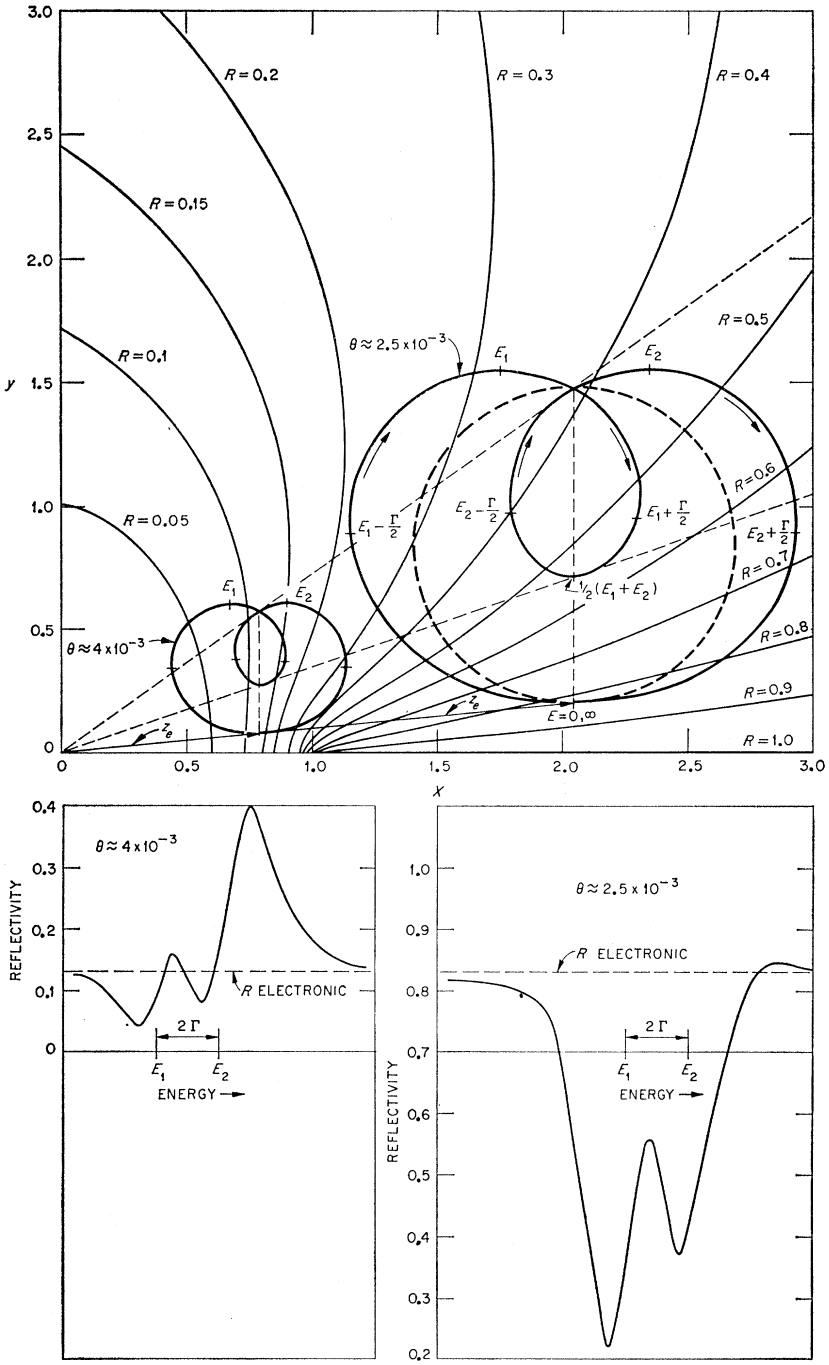

FIG. 1. The upper diagram shows curves of $R(z)=$constant. As the gamma-ray energy goes from 0 to ∞ through the region of two nuclear resonances the values of $z=z_e+z_N$ starts at z_e and traverses the looped curve in a clockwise direction back to z_e. The large curve is for $\theta=2.5\times10^{-3}$, the small one for $\theta=4\times10^{-3}$. The lower curves showing reflectivity versus photon energy for the two angles were derived by reading the contour plot.

in which the complex number $z=x+iy$ is given by

$$z=\frac{2\delta+2i\beta}{\theta^2}=\frac{N\lambda^2}{\pi\theta^2}f(0). \qquad (2)$$

N is the number of scattering centers per unit volume, λ is the wavelength of the radiation, θ is the glancing angle, δ and β are the real and imaginary parts of the complex index of refraction, $n=1-\delta-i\beta$, and $f(0)$ is the complex coherent scattering amplitude per scattering center in the forward direction. β is proportional to the linear absorption coefficient μ by the expression $\beta=(\lambda/4\pi)\mu$, and δ is related to the critical angle for total reflection by $\theta_0=(2\delta)^{\frac{1}{2}}$. A contour plot of R as a function of $z=x+iy$ is given in Fig. 1 by the solid lines each of which is identified with a value $R(z)=c$. For all

values of z along a given contour line the reflectivity R has the value c. For example, the x axis corresponds to absorption $\mu=0$. For all real values of $z>1$, $R=100\%$.

Both transmission and scattering experiments can be described in terms of a complex scattering amplitude. By the optical theorem, the total cross section, which is measured in a transmission experiment, is proportional to the imaginary part of the coherent scattering amplitude in the forward direction, $f(0)$. Coherent scattering processes involve the complex coherent scattering amplitude, both real and imaginary parts. In both transmission and coherent scattering experiments two contributions to the scattering amplitude must be considered: the nonresonant electronic-scattering amplitude f_e; the resonant nuclear-scattering amplitude f_N. The two absolute amplitudes must be added with appropriate phase relations.

In the case of total reflection, by expressions (1) and (2), R depends upon z, which is proportional to (f/θ^2). Consequently, the value of z_e for the electrons must be added to the value of z_N for the Fe^{57} nuclei to form the resultant value $z=z_e+z_N$. The coherent superposition of z_e and z_N is illustrated in the complex plane of Fig. 1. According to the Breit-Wigner expression the value of z_N of a single nuclear resonance is given by the dotted circle shown, the diameter of which has a length equal to the value of z_N at the resonance energy, E_r. The lower end of the vertical diameter of the circle lies at the extreme end of z_e. As the energy E of the incident gamma rays varies from energies much less than E_r to energies much greater than E_r, the resultant z moves clockwise around the circle. For the purpose of illustrating the case of scattering by more than one resonance, we consider the simple case of two resonances at energies E_1 and E_2, having identical full widths Γ and equal strengths, separated by 2Γ. This case is illustrated in Fig. 1 by the solid looped curves. As the energy of the incident photon varies from zero to $+\infty$ the end point of z starts at the end of z_e and tranverses the looped curve in a clockwise direction back to z_e.

The variation of reflectivity with photon energy can be derived from Fig. 1. The curvature, slopes, and spacing of the contour lines differ much in different regions of the plane. The variation of R versus E depends markedly upon the "size" of the looped curve and upon its location in the plane. The glancing angle θ determines the "size," or the "scale factor," of the looped curve, and the region of the complex plane in which the closed curve locus of z falls. The larger looped curve far from the origin corresponds to $\theta\approx 2.5\times 10^{-3}$ rad; the smaller one close to the origin corresponds to $\theta\approx 4\times 10^{-3}$ for the same two resonances. The variation of reflectivity with photon energy E derived by reading the contour plot for each of the two angles is shown qualitatively in the curves below the contour plot of Fig. 1.

These qualitative curves of R versus E derived by reading the contour plot illustrate at once the main optical features of interest. In those regions of energy where R is less than the electronic reflectivity R_e, electronic and nuclear amplitudes interfere destructively; where $R>R_e$ there is constructive interference. This form of interference is relatively more marked for the larger of the two angles. It is constructive at energies greater than the greater resonance energy, and destructive at energies less than the smaller resonance energy. Since the total cross section is proportional to the imaginary part of $f=f_e+f_N$, a transmission experiment would show equal minima near E_1 and E_2 and a maximum halfway between. The minima in transmission are close to the resonance energies because at $|E-E_r|\gg\Gamma$ β falls off quickly as $1/(E-E_r)^2$. Therefore, there may be little interference between he imaginary contributions to f. For scattering, however, there can be strong interference between the real parts δ of the two resonances, since δ varies more slowly as $(E-E_r)/(E-E_r)^2$. The interference effects are more marked for scattering for the additional reason that δ is positive for $E>E_r$ and negative for $E<E_r$, whereas β is always of one sign. Evidence for interference between the two resonance levels in scattering is shown in Fig. 1 by the fact that the minimum at the greater energy lies higher than the minimum at the lower resonance energy.

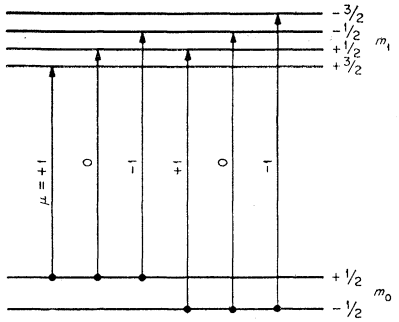

FIG. 2. Energy-level diagram showing Zeeman splitting of the Fe^{57} ground state and 14.4-keV excited state, and the six permitted transitions.

The energy level diagram[7] for the ground state and 14.4-keV isomeric state of Fe^{57} is shown in Fig. 2. The upper state has spin $\frac{3}{2}$, and is split by the magnetic field at the nucleus, due to the spontaneous magnetization of the iron, into four Zeeman levels. The ground state of spin $\frac{1}{2}$ is split into two levels. The selection rules for (magnetic) dipole transitions permit the six transitions shown. Coherent scattering events are those in which an Fe^{57} nucleus is excited by the incoming photon to one of the upper levels and then returns to the level from which it started. Also, the state of the lattice remains unchanged. For a given incident photon energy, all of the six transitions will take place with appropriate probability. All six will contribute to the coherent scattering, each with a phase and magnitude depending on the difference between the incident photon energy and the resonance energy of that transition. The six contributions must be added with appropriate absolute amplitudes and phases.

[7] S. S. Hanna, J. Heberle, C. Littlejohn, G. J. Perlow, R. S. Preston, and D. H. Vincent, Phys. Rev. Letters 4, 177 (1960).

TABLE I. Constants used in numerical calculation of scattering amplitudes and reflectivity.

Incident gamma-ray energy	$=14.4$ keV
Number of nuclei per cm^3 (bulk density)	$=8.47\times10^{22}$
Electronic scattering amplitude:	$f_e=(6.30\times10^{-12}\text{ cm})+i(6.30\times10^{-13}\text{ cm})$
Total natural linewidth,	$\Gamma=4.60\times10^{-9}$ eV
Width for gamma emission	$\Gamma_i=1/16\Gamma$
Angular resolution: full width at $\frac{1}{2}$-max	$=0.57\times10^{-3}$ rad
Width of gamma source: full width at $\frac{1}{2}$-max	$=11.50\times10^{-9}$ eV
Relative abundance of Fe^{57} in the mirror, (E)	$=91.2\%$
$1-F=e^{-k_0^2\langle x^2\rangle}$	$=0.7$

The nuclear coherent scattering amplitudes for the case of magnetic dipole scattering are given by the following expression of Trammell[8]:

$$f_{m,m'}=\frac{E}{(2j_0+1)}\sum_{m_0}\sum_{\mu}\tfrac{3}{2}D_{\mu m'}^{(1)*}(\hat{k}_f,\hat{Z})D_{\mu m}^{(1)}(\hat{k}_0,\hat{Z})\times C^2(j_0 1 j_1; m_0\mu)\frac{\Gamma_i}{2k_0}\frac{e^{-k_0^2\langle x^2\rangle}}{E_{k_0}-E_r(m_0,m_0+\mu)+i\frac{1}{2}\Gamma}. \quad (3)$$

In (3) E is the enrichment of Fe^{57}, $\hat{k}_0$ is a unit vector in the direction of propagation of the incident gamma ray, $\hat{k}_f$ is a unit vector in the direction of the scattered photon, $\hat{Z}$ is a unit vector in the direction of the magnetic field at the scattering nucleus, C is the appropriate Clebsch-Gordan coefficient, k_0 is the wave number of the photons, Γ_i is the width of the 14.4-keV Fe^{57} level for gamma emission, $e^{-k_0^2\langle x^2\rangle}$ is the factor multiplying the amplitude to take account of the fact that only a fraction of the radiation is scattered without energy loss, E_{k_0} is the energy of the photons, E_r the resonance energy, Γ the total width of the 14.4-keV level. m is the circular polarization of the incident photon, m' is the circular polarization of the outgoing photon ($m,m'=\pm1$ for right or left circularly polarized light), j_0 and j_1 are the spins of the ground and excited states, respectively. m_0 is the Z component of the spin of the ground state ($\pm\frac{1}{2}$). In (3) $\mu=\pm1$ corresponds to right- and left-hand circular oscillators, $\mu=0$, to a linear oscillator along the $\hat{Z}$ axis. $D_{\mu m'}^{(1)*}$, and $D_{\mu m}^{(1)}$ give the angularly dependent excitation and emission factors for these oscillators. These matrix elements of the rotation operator are given in terms of the appropriate Euler angles. The notation for the rotation operator matrix elements and the Clebsch-Gordan coefficients is that of Rose.[9]

For a given pair of incident and scattered polarizations the double sum of (3) contains six terms, one for each of the six lines. There are four such possible pairs of circular polarizations. For each incident gamma-ray energy these four numbers ($f_{1,1}$, $f_{1,-1}$, $f_{-1,1}$, $f_{-1,-1}$) constitute a matrix which multiplies the vector of incident amplitudes to give the scattered amplitudes, all in terms of circular polarization. The outgoing amplitudes A_+', A_-' are given in terms of the incident amplitudes by

$$\begin{pmatrix}A_+'\\A_-\end{pmatrix}=\begin{pmatrix}f_{1,1} & f_{1,-1}\\ f_{-1,1} & f_{-1,-1}\end{pmatrix}\begin{pmatrix}A_+\\A_-\end{pmatrix}. \quad (4)$$

In (4) the + sign denotes right circular polarization, the negative sign left circular polarization.

For forward scattering $\hat{k}_0=\hat{k}_f$. We consider two cases for $\hat{Z}$: (1) No magnetic field is applied to the mirror. In this case we assume that the spontaneous magnetization vectors of the domains of the Fe^{57} film lie in the plane of the mirror surface, all directions in this plane being equally probable. Each of the four amplitudes must be averaged over such a distribution. (2) The magnetic field at the Fe^{57} nuclei is assumed to be perpendicular to $\hat{k}_0$ and to lie in the plane of the mirror. In both cases (1) and (2), $f_{1,1}=f_{-1,-1}$ and $f_{1,-1}=f_{-1,1}$.

In using expression (1), R must be calculated for each of the two linear polarization states separately and averaged. In terms of linear polariaztions, the matrix equation (4) becomes

$$\begin{pmatrix}A_1'\\A_2'\end{pmatrix}=\begin{pmatrix}f_{1,1}-f_{1,-1} & 0\\ 0 & f_{1,1}+f_{1,-1}\end{pmatrix}\begin{pmatrix}A_1\\A_2\end{pmatrix}. \quad (5)$$

In (5) A_1', A_1 are identified with the polarization in which the electric field E is parallel to the scattering plane (perpendicular to the mirror), and A_2', A_2 with E perpendicular to the scattering plane (parallel to the plane of the mirror). The incident beam is unpolarized. Therefore, $|A_1|=|A_2|$, and each can be taken equal to one. A_1' and A_2' are the nuclear contributions to the scattering amplitude $f(0)$ in expression (2) above.

A certain fraction F of the intensity emitted by the source suffers a change in energy due to phonon gain or loss on emission. This fraction will not be resonantly scattered by the Fe^{57} nuclei in the mirror but will be scattered by the electrons of the mirror. The reflectivity is, therefore, given by

$$R=R_eF+(1-F)[\tfrac{1}{2}(R_1+R_2)] \quad (6)$$

in which R_e is the reflectivity due to electrons alone, R_1 and R_2 the reflectivities due to both Fe^{57} nuclei and electrons for the electric field E, respectively, parallel and perpendicular to the scattering plane.

[8] G. T. Trammell, Phys. Rev. **126**, 1045 (1962).
[9] M. E. Rose, *Elementary Theory of Angular Momentum* (John Wiley & Sons, Inc., New York, 1957).

TABLE II. Values of Clebsch-Gordan coefficients, C^2 for nuclear transitions in Fe^{57}.

m_0	μ 1	0	−1
$+\frac{1}{2}$	1	$\frac{2}{3}$	$\frac{1}{3}$
$-\frac{1}{2}$	$\frac{1}{3}$	$\frac{2}{3}$	1

CALCULATIONS

The computation of the scattering amplitudes and reflectivities were made using the constants given in Table I. The values of the Clebsch-Gordan coefficients for the Fe^{57} transitions are given in Table II.

Using (3) and (5) and the constants given, the expressions for A_1' and A_2' become

$$A_1'=f_{1,1}-f_{1,-1}=0.855\times10^{-12}\text{ cm}\times\sum_{m_0,\mu}A_{m_0,\mu}\Big/\left(\frac{E_{k_0}-E_r}{\frac{1}{2}\Gamma'}+i\right),\quad(7)$$

$$A_2'=f_{1,1}+f_{1,-1}=0.855\times10^{-12}\text{ cm}\times\sum_{m_0,\mu}B_{m_0,\mu}\Big/\left(\frac{E_{k_0}-E_r}{\frac{1}{2}\Gamma'}+i\right).\quad(8)$$

TABLE III. Values of $A_{m_0,\mu}$, $B_{m_0,\mu}$ for ferromagnetic Fe metal, random magnetic field directions in plane of mirror.

	$m_0=+\frac{1}{2}$			$m_0=-\frac{1}{2}$		
μ	1	0	−1	1	0	−1
A	3	4	1	1	4	3
B	6	0	2	2	0	6
Source velocity[a] cm/sec	−0.523	−0.298	−0.074	0.095	0.319	0.544

[a] The values of source velocity are based on those given by S. S. Hanna, R. S. Preston, and J. Heberle, in *Proceedings of the Second International Conference on the Mössbauer Effect, Saclay, France, 1961* (John Wiley & Sons, Inc., New York, 1961), p. 85.

Values of $A_{m_0,\mu}$ and $B_{m_0,\mu}$ to be used in (7) and (8) for ferromagnetic Fe^{57} metal are given in Table III for the case of H random in the mirror plane, and in Table IV for $H\perp k_0, k_f$. The value of linewidth Γ' to be used in (7) and (8) is four times the natural width. The use of this value of Γ' reduces the nuclear amplitude to one-fourth of that corresponding to the natural width [Eq. (3)]. The values of R calculated from (1), (2), (6), (7), and (8) are shown in Figs. 3, and 4(a'), 4(b'), 4(c'), as a function of source velocity v. The photon energy $h\nu$ (velocity v) is related to photon energy $h\nu_0$ (velocity zero) by the Doppler expression, $E_{k_0}=h\nu=h\nu_0(1+v/c)$. Corrections were applied for the angular spread of the rays due to the finite size of source and detector, and for the frequency width of the source. The positions of the lines which would be observed by transmission through Fe^{57} are shown by the vertical arrows along the axis of abscissae. Figures 3 and 4(b') are calculated for an unmagnetized ferromagnetic Fe^{57} metal mirror. The six lines correspond to the six permitted transitions in Fe^{57}.

TABLE IV. Values of $A_{m_0,\mu}$, $B_{m_0,\mu}$ for ferromagnetic Fe metal, $H\perp\hat{k}_0,\hat{k}_f$.

	$m_0=+\frac{1}{2}$			$m_0=-\frac{1}{2}$		
μ	1	0	−1	1	0	−1
A	0	8	0	0	8	0
B	6	0	2	2	0	6
Source velocity cm/sec	−0.523	−0.298	−0.074	0.095	0.319	0.544

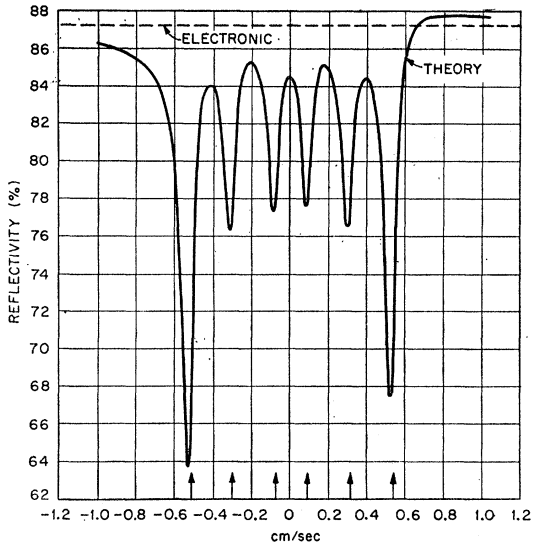

FIG. 3. Calculated reflectivity R versus velocity v for $\theta=2\times10^{-3}$ rad, $H=0$, for 6 transitions of ferromagnetic Fe^{57} metal.

Figures 3 and 4(b') exhibit the interference between the contributions to the nuclear-scattering amplitude from the transitions between the various nuclear Zeeman levels, and the interference between the nuclear and electronic scattering. The effects of electronic and nuclear interference are quite similar to those described abovef or two equal resonances. The effects of interference between levels are somewhat more complicated for the six line spectrum than for the two line spectrum. In Fig. 4(a) the outermost minimum R on the left (corresponding to $\mu=+1$, $m_0=+\frac{1}{2}$) lies deeper than the right-hand outermost minimum ($\mu=-1$, $m_0=-\frac{1}{2}$). This behavior of corresponding lines at positive and negative velocities is due to interference of the scattering amplitudes from the several transitions between the Zeeman levels of excited and ground states of Fe^{57}. The displacements of the maxima and minima from the resonance energies due to interference between transitions and to the character of the contour map are more apparent in Fig. 4(b') for $\theta=4\times10^{-3}$ than in Fig. 3 for $\theta=2\times10^{-3}$.

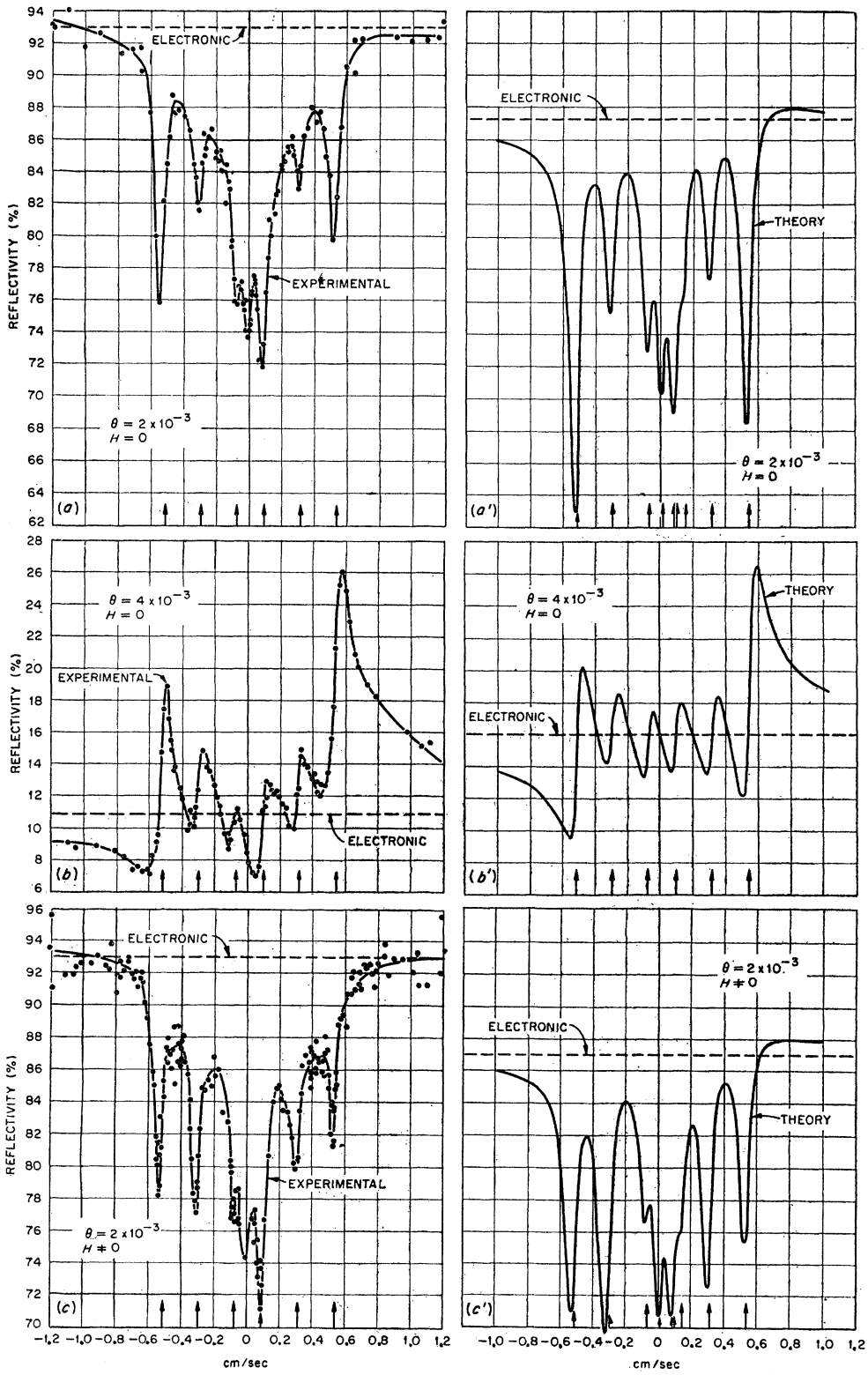

FIG. 4. Reflectivity R versus velocity v for various glancing angles and applied magnetic field. Left-hand curves give measured values of R. Right-hand curves give calculated values. (a), (a′) for $\theta=2\times10^{-3}$ rad, $H=0$; (b), (b′) for $\theta=4\times10^{-3}$ rad, $H=0$; (c), (c′) for $\theta=2\times10^{-3}$ rad, magnetic field in plane of mirror perpendicular to propagation vector.

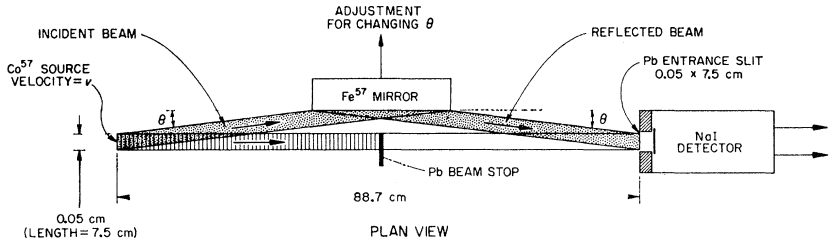

FIG. 5. Schematic diagram of apparatus for the measurement of the intensity of 14.4-keV Fe^{57} gamma rays reflected from an Fe^{57} mirror.

TABLE V. Strengths of additional lines.

Resonance velocity cm/sec	A	B
0.010	2	2
0.083	1.5	1.5
0.147	1.5	1.5

If resonance lines in addition to the six line spectrum of ferromagnetic Fe^{57} metal were present, due to the presence in the film of Fe^{57} in a nonferromagnetic state the presence of the additional lines would affect the reflectivity curves in detail, but would not affect the character of those features of the curves related to the two types of interference. In Figs. 4(a′) and 4(c′), in order to obtain better agreement in detail of the calculated R versus v curves with the measured curves, three lines at 0.010, 0.083, and 0.147 cm/sec have been added to the usual six line Fe^{57} spectrum with the A and B strength factors of Table V.

APPARATUS

The experimental arrangement is shown schematically in Fig. 5. A long narrow source was prepared by electroplating about 300 mCi of Co^{57} on the 7.5-cm $\times$0.05-cm face of a 302 stainless steel plate. The plate was then annealed in a hydrogen atmosphere at 1000°C for 2 h, giving a single line source of the 14.4-keV Fe^{57} gamma radiation. The reflecting surface of the mirror consisted of a thickness of about 150 Å of 91.2% enriched Fe^{57} evaporated upon a 30-cm$\times$10-cm optically flat surface of a Pyrex plate, 2 in. thick. The gamma-ray detector was a plate of NaI about 0.020 in. thick. The width of the entrance slit to the detector was the same as the source width, 0.05 cm, and about the same length. The source could be moved at any chosen uniform velocity by means of a commercial air-motor with adjustable oil damping to control the speed in each direction. Measurements were taken of the gamma-ray intensity reflected by the mirror as a function of glancing angle and velocity. The number of counts in each of the two directions of velocity were recorded in every cycle cumulatively in corresponding scaling circuits. Times were measured with a 1000-cycle oscillator. The direct beam from the source to the detector slit was eliminated by the lead stop shown. The angle of incidence was varied by translating the mirror a measured distance parallel to itself in a direction perpendicular to the direct beam. Since the mirror was symmetrically located between source and detector, the specularly reflected beam reaches the detector. The angular width of the beam from the source accepted by the detector was 0.57×10^{-3} rad, full width at half-maximum. Accurate alignment of the apparatus was achieved by the use of optical levers with visible light, and by use of measurements of the direct beam gamma-ray intensity. The absolute value of the reflectivity R is given by the ratio of the intensity of 14.4-keV gamma radiation in the reflected beam to that in the direct beam. A single-channel pulse-height selector was used in connection with the NaI detector to measure the intensity of the gamma rays. The data were taken with the center of the window of the pulse-height selector set on the 14.4-keV peak due to the transition from the 10^{-7} sec isomeric level to the ground state of Fe^{57}. Pulses at this setting due to the 137-keV gamma ray of Fe^{57} and 6.4 keV x ray of Fe were taken account of by the use of several aluminum absorbers. Proper account must be taken of the nonresonant radiation, since the energy spectrum is considerably different in the direct and reflected beams. Source and scatterer were at room temperature.

RESULTS AND MEASUREMENTS

The reflectivity R was measured as a function of glancing angle θ and source velocity v. R as a function of θ is shown in Fig. 6 for velocities 0, +0.6, −0.6, and

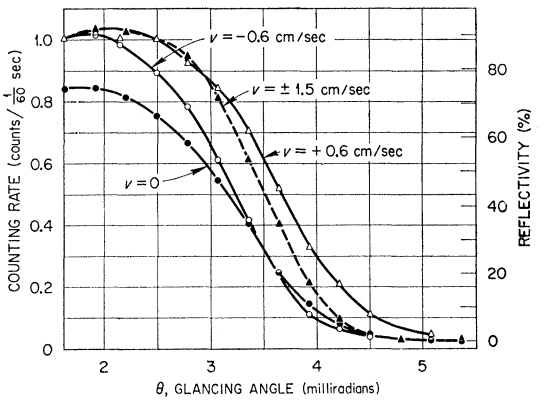

FIG. 6. Reflectivity R versus glancing angle θ for source velocities 0, +0.6, −0.6, and ±1.5 cm/sec.

± 1.5 cm/sec. R versus v is shown for $\theta = 2\times10^{-3}$ rad in Fig. 4(a), and for $\theta = 4\times10^{-3}$ rad in Fig. 4(b). R versus v for $\theta = 2\times10^{-3}$ rad for the case of the magnetic field perpendicular to the propagation vector is shown in Fig. 4(c). The velocities at which lines are found in transmission experiments of ferromagnetic Fe metal are shown by the arrows. Statistically each of the relative values of R has a probable error of 0.007 R, absolute R's may be shifted by 0.01 R. Similarly, the scale of angle may be shifted from one run to another by as much as 0.1 mrad, but the error in angle difference of a single run does not exceed 0.02 mrad.

COMPARISON OF MEASUREMENTS AND CALCULATIONS

The measured curves of R versus v of Fig. 4 show clearly evidence for the two types of interference, between scattering from electrons and nuclei and between the several nuclear transitions, discussed above for the illustrative two line spectrum and for the calculated patterns of the 6 line ferromagnetic Fe^{57} spectrum of Figs. 3 and 4(b′). It is evident also from Figs. 4(a) and 4(c) that the data show resonances in addition to the 6 lines. Figures 4(a) and 4(c) show a line at velocity close to zero which is not present in the calculated curve of Fig. 3 for a ferromagnetic Fe^{57} metal mirror. We suspect that actually two extra lines appear in the data, the second being an unresolved doublet centered at about 0.11 cm/sec. Since FeO is a likely contaminant in the film, the additional strength of resonance required near 0.11 cm/sec can perhaps be assumed to be due to FeO, which shows an electric quadrupole doublet with lines at 0.083 and 0.146 cm/sec.[10] The line near zero velocity can perhaps be attributed to the presence in the film of nonmagnetic gamma iron. The existence of (paramagnetic) gamma iron at room temperature has been inferred from Mössbauer transmission experiments through small particles of iron precipitated in a matrix of copper.[11] In the calculations of Fig. 4(a′) and 4(c′) lines at 0.083, 0.146, and 0.010 cm/sec with the strengths shown in Table V have been added to the 6 line ferromagnetic Fe^{57} spectrum. Comparison of Figs. 3, 4(a), and 4(a′) shows that the correspondence between measured and calculated curves for $\theta = 2\times10^{-3}$ is improved in detail by the contribution of the three additional lines. In the calculation it was assumed that the origins of these transitions were homogeneously distributed in the film and that the entire spectrum of nine lines scattered coherently. The additional three lines were not included in the calculations of Fig. 4(b′) for glancing $\theta = 4\times10^{-3}$, since the data of Fig. 4(b) show no need for them. Their omission in this case seems reasonable since the penetration depth at $\theta = 4\times10^{-3}$ is much greater than at $\theta = 2\times10^{-3}$. If the oxide exists mostly near the surface, then the scattering from it will contribute relatively much less at the larger angle.

The changes produced in the spectra by the applied magnetic field $H \perp \hat{k}_0$ can be seen by comparing Figs. 4(c), 4(c′) for $H \neq 0$ with Figs. 4(a), 4(a′) for $H = 0$. The shapes of the measured curves are changed by the application of the field in accord with theory. For example the minima of the two adjacent outermost pairs of lines at positive or negative velocities are quite different for $H = 0$ but nearly equal for $H \neq 0$.

In Fig. 4 the values of R_e of the calculated curves was determined using the crystal density of iron metal and values of δ and β for the electrons from x-ray measurements. The values of R_e of the measured curves were determined from measurements of R at velocities far outside the resonance region. No normalization of R_e calculated to R_e measured was made. With respect to the variations of R about R_e for the calculated curves, the only parameter adjusted was the linewidth of the excited state of Fe^{57} of the mirror. In view of the decision not to adjust any parameters except the linewidth and in view of the difficulty of the measurements, the agreement between the curves of measured and calculated R versus v is very gratifying.

A puzzling feature of the data is the fact that the lines of the measured curves of Fig. 4(a) [and also 4(c)] seem to hang from a sagging base line, whereas the lines of the calculated curves of Figs. 3 and 4(a′) hang from the horizontal asymptotic base line of value R_e. Intuitively it seems as though a very broad resonance of about 0.3 cm/sec width may exist in the data. We have calculated the effect on the reflectivity of a transition layer in which the magnetic field at the Fe^{57} nuclei varies linearly from zero at the film surface to its saturation value at a certain depth in the film. (Magnetic measurements of some ferromagnetic films have been interpreted in terms of a transition layer in which the magnetization is less than the bulk value.[12] The calculations show that the effect of such a layer on the scattering is indeed much like that of a very broad resonance of the required width, having real and imaginary parts of the scattering amplitudes which are distorted from but roughly similar to the Breit-Wigner shapes. The difficulty is that a broad resonance, because of the characteristics of the reflectivity contour lines, introduces an asymmetry between the reflectivities at corresponding positive and negative velocities which does not exist in the "big dip" suggested by the data.

The differences in line structure between the measurements and the curves calculated on the assumption of a 6-line ferromagnetic film of Fe^{57} metal emphasize the fact that in the region of total reflection only a very small thickness of the mirror is effective. The penetration depth is perhaps 20Å or less for a glancing angle of 2×10^{-3} rad. The technique of total reflection of nuclear

[10] G. Shirane, D. E. Cox, and S. L. Ruby, Phys. Rev. **125**, 1158 (1962).

[11] U. Gonser, C. J. Meechan, A. H. Muir, and H. Wiedersich, Bull. Am. Phys. Soc. **7**, 600 (1962).

[12] W. Reincke, Z. Physik **137**, 169 (1954).

resonance radiation should, therefore, be very useful for studying the magnetic and chemical states of very thin surface layers.

ACKNOWLEDGMENTS

We are grateful to J. J. Pinajian for supervision of the preparation of the Ni target and its bombardment in the cyclotron for the purpose of producing Co^{57}, to G. W. Parker for extraction of the Co^{57} and electroplating it on stainless steel, to S. A. Rabin for annealing the source, to C. W. Nestor, Jr., for help with the computer calculations, to L. Owens and W. G. Mankin for help in taking the data, to H. L. Adair for preparation of the Fe^{57} mirror, and to G. T. Trammell, T. A. Welton, and R. L. Becker for valuable discussions of theoretical aspects of the experiment.

PHYSICAL REVIEW VOLUME 132, NUMBER 4 15 NOVEMBER 1963

Free-Positron Annihilation Mean Life in Diatomic and Rare Gases in Liquid and Solid States

D. C. Liu and W. K. Roberts
Lewis Research Center, National Aeronautics and Space Administration, Cleveland, Ohio
(Received 8 July 1963)

Measurements have been made on the free-positron annihilation mean life, τ_1, in H_2, D_2, He, N_2, O_2, Ne, Ar, and Xe in liquid and/or solid states. To a fair approximation, the observed mean lives may be represented by the equation: $\tau_1(\text{nsec}) = 0.31 + 0.15 \times 10^{-4}\, E_i^2/\rho_e$, where E_i is the first electron ionization potential in eV, and ρ_e is the number of outermost electrons per unit "atomic volmue" a_0^3. In the H_2 and D_2 isotopes where E_i is constant, τ_1 is linearly dependent on ρ_e^{-1}. It was also found that τ_1 is independent of the ortho-para ratio of the liquid H_2 at 20.4°K.

INTRODUCTION

In a previous report[1] it was shown that the observed free-position annihilation mean life, τ_1, has a linear dependence on the ratio of the first electron ionization potential to the outermost electron density, E_i/ρ_e, for liquid H_2, N_2, and O_2. It was noted, however, that the observed τ_1 in liquid He is 30% larger than the value expected from this relationship. In an effort to look for a consistent relationship among the values of τ_1 in rare and diatomic gases, the measurements were extended to other rare gases. This paper presents the results of a further investigation concerning the dependence of τ_1 in condensed elementary gases on E_i and ρ_e.

When positrons are used to study the electronic structure of solids, it must be remembered that the presence of positrons in the solid affects the electronic configuration. On the other hand, the positrons would cause the same perturbation in each member of a pair of isotopes. The use of H_2 and D_2 made possible an examination of the dependence of τ_1 on ρ_e at constant E_i. Measurements were also made on the τ_1 in liquid H_2 of different ortho-para ratios at constant temperature.

APPARATUS

"Research Grade" gaseous D_2, O_2, Ar, and Ne purchased from the Matheson Company were liquefied and/or solidified in a $1\frac{1}{8}$-in. diam by 5-in. evacuated stainless-steel chamber submerged in a cryogenic liquid bath of appropriate temperature. Gaseous Xe, also of "Research Grade," was solidified in a $\frac{1}{2}$-in. diam by 2-in. chamber submerged in a liquid-nitrogen bath. A small quantity of isotopically pure Na^{22} was sandwiched between 0.0001-in.-thick rubber-hydrochloride films, supported by an aluminum frame, and radially centered in each chamber.

The delayed-coincidence apparatus used in I was further improved by the addition of auxiliary electronics. The dewar system necessitated a 2-in. separation between the positron source and the front surface of each detector. A slow signal for energy discrimination was taken from the tenth dynode of each 56 AVP photomultiplier tube and routed to an amplifier-discriminator system. One slow discriminator was set to accept the upper 40% of the nuclear gamma-ray Compton spectrum, while another discriminator was set with a window to accept the upper 30% of the positron annihilation gamma-ray Compton spectrum. The fast anode pulse from each photomultiplier tube was limited by a tunnel diode (1N2939) and used to trigger a tunnel diode univibrator. The univibrator pulse was used to turn off an npn transistor (2N797) that was normally in saturation. The fast square positive pulses thus produced were sent to a time-to-pulse height converter (hereafter referred to as TPHC) of Simms' design.[2] The TPHC output was sent to a 400-channel pulse-height analyzer for gating and storage. The gating system used was similar in principle to that described by Schwarzchild,[3] in that it

[1] D. C. Liu and W. K. Roberts, Phys. Rev. **130**, 2322 (1963); hereinafter this is referred to as I.

[2] P. C. Simms, Rev. Sci. Instr. **32**, 894 (1961).

[3] A. Schwarzchild, Nucl. Instr. Methods **21**, 1 (1963).